Original article

Three new spirocyclic terpenoids from *Euphorbia amygdaloides* exhibit cytotoxicity against cancerous cell lines through early and late apoptosis

Ardalan Pasdaran [a,b,e], Negar Azarpira [c], Mahdokht Hossein Aghdaie [c], Maryam Zare [d,e], Negin Sheidaie [d,e], Fatemeh Hajeb Fard [d,e], Azadeh Hamedi [a,e,*]

[a] *Medicinal Plants Processing Research Center, Shiraz University of Medical Sciences, Shiraz, Iran*
[b] *Phytopharmaceutical Technology and Traditional Medicine Incubator, Shiraz University of Medical Sciences, Shiraz, Iran*
[c] *Transplant Research Center, Shiraz University of Medical Sciences, Shiraz, Iran*
[d] *Student Research Committee, School of Pharmacy, Shiraz University of Medical Sciences, Shiraz, Iran*
[e] *Department of Pharmacognosy, School of Pharmacy, Shiraz University of Medical Sciences, Shiraz, Iran*

ARTICLE INFO

ABSTRACT

Bioassay-guided fractionation led to the isolation of three new spirocyclic terpenoid compounds from *Euphorbia amygdaloides* L., named Zagrosin I–III. Their structures were identified by 1D and 2D NMR (^{1}H NMR, ^{13}C NMR, DEPT 135, HMBC, and HSQC-TOCSY) and LC-MS-MS spectrometry. The cytotoxicity of the isolated spirocyclic terpenoids (Zagrosin I-III) was assessed against human breast cancer (MCF-7), human fibrosarcoma (HT1080), and normal human foreskin fibroblast cells with MTT assays (24, 48, and 72 h treatments). The FITC-Annexin V apoptosis flow cytometry assays and cell cycle analysis were performed for Zagrosin I–III.

These isolated compounds were identified as: (9)-8a-((benzoyloxy)methyl)-2-methoxy-4,9-dimethyltetrahydro-4H,5H-2,4a-methanobenzo[d] [1,3] dioxine-4-carboxylate (Zagrosin I), ((9)-4-hydroxy-2-methoxy-4,9-dimethyltetrahydro-4H,8aH-2,4a-methanobenzo[d] [1,3] dioxin-8a-yl) methyl benzoate (Zagrosin II), and (9)-2-methoxy-4,9-dimethyl-8a-(phenoxy methyl) tetrahydro-4H,5H-2,4a-methanobenzo[d][1,3]dioxin-4-yl 4-methyl-pentanoate (Zagrosin III).

The IC$_{50}$ of Zagrosin I on 48-h-treated MCF-7 was calculated as 1.5 µg/mL. Zagrosin II and III exhibited cytotoxicity on 48-h-treated MCF-7 with IC$_{50}$s of 14.04 and 12.50 µg/mL, respectively. The IC$_{50}$ of Zagrosin I on human fibrosarcoma (HT1080) was 115.5 µg/mL, Zagrosin III, 16.81 µg/mL (48 h treatment), and Zagrosin II, 142.7 µg/mL (72 h treatment). Zagrosin I-III exhibited significant cytotoxicity against the MCF-7 cell line and human fibrosarcoma (HT1080), with the mechanism of early and late apoptosis affecting cells mostly in G0/G1 fallowed by S and G2 phases. MCF-7 had a higher rate of phosphatidyl serine exposure on the cell membrane than two other studied cells. The cytotoxicity on normal human foreskin fibroblasts was low. Zagrosin I-III can be considered an effective chemical backbone for anticancer drug development.

Abbreviations: 2D NMR: Two-Dimensional Nuclear Magnetic Resonance Spectroscopy; API: Atmospheric Pressure Ionization; DEPT: Distortionless Enhancement by Polarization Transfer; ELISA: Enzyme-Linked Immunosorbent assay; ERK: Extracellular signal-regulated kinase; ESI: Electrospray ionization; FBS: Fetal Bovine Serum; FITC: Fluorescein isothiocyante; fr: fraction; HMBC: Heteronuclear Multiple Bond Correlation; HPLC: High-Performance Liquid Chromatography; HSQC: Heteronuclear Single Quantum Coherence; HT1080: Human fibrosarcoma cell line; IC$_{50}$: Half-maximal inhibitory concentration; MCF-7: Human breast cancer cell line; MHz: Megahertz; MTT: 3-[4,5-dimethylthiazol-2-yl]-2,5 diphenyl tetrazolium bromide; NMR: Nuclear Magnetic Resonance; PBS: Phosphate Buffered Saline; PI: Propidium Iodide; ppm: Part Per Million; R$_f$: Retention Factor; TLC: Thin-layer chromatography; TOCSY: Total Correlation Spectroscopy; VLC: Vacuum Liquid Chromatography.

* Corresponding authors at: Department of Pharmacognosy, School of Pharmacy, Shiraz University of Medical Sciences, Shiraz, P.O. Box: 7146864685, Iran.
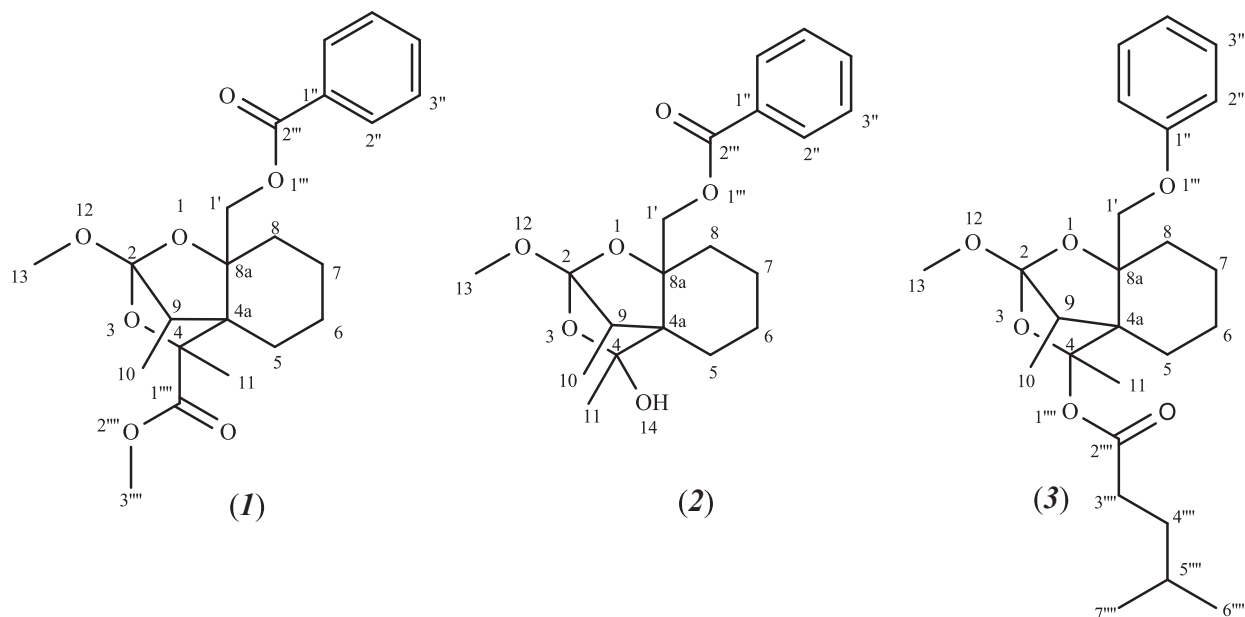*E-mail address:* hamediaz@sums.ac.ir (A. Hamedi).

Fig. 1. Chemical structures of Zagrosin I-III (*1–3*).

1. Introduction

The long ethnomedicinal history, ethnopharmacological applications, and diverse metabolite content of the Euphorbiaceae family make this plant family a precious source for phytochemistry and drug discovery studies (Hamedi et al. 2022; Ernst et al. 2015; Amtaghri et al. 2022; Benjamaa et al. 2022). Plants of this family are well-known as popular traditional remedies in the treatment of cancer, inflammation, skin diseases, and infectious diseases. Many pieces of evidence have shown that different parts of various Euphorbia plants, such as stem barks, latex, seeds, and leaves, have been used medicinally (Kemboi et al. 2020b; Pascal et al. 2017). Although many regional therapeutic uses are related to the endemic Euphorbia species, some of the most frequently used species in the Mediterranean and Middle East include *Euphorbia myrsinites* L., *Euphorbia macroclada* Boiss., *Euphorbia seguieriana* Necker., and *Euphorbia peplus* L (Özbilgin and Gülçin 2012; Moghaddas et al. 2017). The Euphorbia genus is a rich source of terpenoid molecules such as myrsinols, lathyranes, ingenanes, cembranes, tiglianes, jatrophane, abietanes, and daphnanes. A variety of diterpenes from the Euphorbia genus have been reported as potential leads for drug development studies. Several diterpenoids, including jatrophane, modified jatrophane, segetane, pepluane, and paraliane, were extracted, purified, and described from *Euphorbia dendroides*, *Euphorbia characias*, *Euphorbia peplus*, *Euphorbia amygdaloides*, and *Euphorbia paralias*. Among them, fifty diterpenoids were reported for the first time (Barile, Corea, and Lanzotti 2008). Moreover, a number of diterpenes named amygdaloidins (A-L) have been isolated from *E. amygdaloides* (Barile, Corea, and Lanzotti 2008; Corea et al. 2005). Diterpenoids have been reported for a diverse range of pharmacological properties, including anti-inflammatory, antiviral activities, and cytotoxicity. Several types of diterpenoids were reported from this genus, such as isopimarane, rosane, abietane, ent-kaurane, and ent-atisane. cembrane, casbane, lathyrane, myrsinane, jatropholane, tigliane, ingenane, jatrophane, paraliane, pepluane, and euphoractin (Zhao et al. 2022). Researchers have also reported triterpenoids from the Euphorbia genus. These triterpenoids mostly belonged to the tirucallane, cycloartanes, lupane, oleanane, ursane, and taraxane subclass. The majority of them exhibit significant cytotoxic and anticancer activities (Kemboi et al. 2020a).

Besides phytochemical diversity, terpenoids provide a promising source for investigating small molecules with cytotoxic and anticancer properties. A successful example of a naturally derived diterpene drug is taxol. As another distinct example, a diterpene of E. peplus, ingenol metabutate (picato®), can be mentioned, which is an FDA-approved drug in actinic keratosis treatment (Ogbourne and Parsons 2014). The isolated flavonoids form *Euphorbia* spp. exhibited anticancer, anti-proliferative, antimalarial, antibacterial, anti-venom, anti-inflammatory, anti-hepatitis, and antioxidant properties and shown different mechanisms of action against cancer cells (Magozwi et al. 2021). Some flavonol glycosides have also been reported from *E. amygdaloides* (Müller and Pohl 1970).

E. amygdaloides is a perennial herb (30–60 cm tall) with mahogany-red leathery leaves (6 cm long) and glabrous, smooth, spherical seeds. In this research, the cytotoxic properties of *E. amygdaloides* fractions, and the most effective constituents were investigated based on the bioassay guided fractionation method. The chemical structure of these isolated compounds was determined based on the various 1D NMR (^{1}H NMR, ^{13}C NMR, Dept-135), 2D NMR (HMBC, HSQC-TOCSY), and mass spectrometry techniques.

2. Materials and methods

2.1. Plant, cells, and other materials

E. amygdaloides aerial parts, including leaves and stems, were gathered during October from the Pooladkaf zone near Sepidan county in the northwest of Fars province with 30°20′15.3″N 51°57′38.5″E geographical directions and an altitude of 2809 m. This plant was established at the Medicinal Plants Processing Research Centre, Shiraz University of Medical Sciences, Shiraz, Iran, by Dr. Ardalan Pasdaran with a voucher specimen (MPPRC-99–2).

Human breast cancer (MCF-7) and human fibrosarcoma cells (HT1080) were purchased from the Pasteur Institute (Tehran, Iran). The human foreskin fibroblasts were obtained from the Transplant Research Center (Shiraz, Iran). Solvents were of high purity and purchased from Dr. Mojallali Industrial Chemical Complex Co. (Tehran, Iran). All other chemicals were purchased from Sigma-Aldrich (USA) or Merck (Merck Millipore, Germany). Trypsin was purchased from Gibco (Italy).

2.2. Extraction and isolation

Dried *E. amygdaloides* aerial parts (2.3 kg) were macerated and extracted with hexane, dichloromethane, and methanol (10 L of each

Table 1
^{1}H NMR, ^{13}C NMR, Dept-135, HMBC, and HSQC-TOCSY data of Zagrosin I (**1**).

Position number	Hetero atom	^{1}H NMR	^{13}C NMR	Dept-135	HMBC (H → C)	HSQC-TOCSY
1	O	–	–	–	–	–
2		–	– (q)	–	–	–
3	O	–	–	–	–	–
4		–	– (q)	–	–	–
4a		–	– (q)	–	–	–
5		1.35	28.90 (s)	28.90	11, 9, 8, 1′	6, 8, 9, 10, 1′, 7, 11
6		0.82, 1.34 §	22.98 (s)	22.98	8, 10, 7	7, 5, 8, 1′
7		1.24§	23.69 (s)	23.69	6, 5	6, 5, 8, 9, 1′
8		0.82, 1.34 §*	30.31 (s)	30.31	11, 1′, 9	11, 9, 7, 5, 6, 1′
8a		–	– (q)	–	–	–
9		1.68 §	38.67 (t)	38.67	1′, 5	1′, 10, 5, 7, 11
10		0.85	10.94 (p)	10.94	–	6, 8, 9,1′
11		1.25–1.32§*	14.06 (p)	14.06	5, 8	10, 6, 5,8
12	O	–	–	–	–	–
13		3.69*	50.64 (p)	50.64	–	–
1′a		4.20 (dd)	68.20 (s)	68.20	7, 5, 9, 2‴	10, 8, 7, 5, 6, 9
1′b		4.14 (dd)				
1″		–	132.36 (q)*	–	–	–
2″		7.60–7.65*	130.94 (t)*	130.94	6″, 2‴	3″, 4″, 5″, 6″
3″		7.43–7.45*	128.79 (t)*	128.79	6″, 5″	2″, 4″, 6″, 5″
4″		7.43–7.45*	128.79 (t)*	128.79	6″, 2″	2″, 3″,5″, 6″
5″		7.43–7.45*	128.79 (t)*	128.79	3″, 6″	3″, 2″, 4″, 6″
6″		7.60–7.65*	130.94 (t)*	130.94	2″, 2‴	2″, 3″,5″, 4″
1‴	O	–	–	–	–	–
2‴		–	167.82 (q)	–	–	–
1⁗		–	161.56 (q)	–	–	–
2⁗	O	–	–	–	–	–
3⁗		3.69*	50.92 (p)	50.92	1⁗	–

§ Assigned and confirmed based on Dept-135, HMBC and HSQC-TOCSY data.
* Overlapped peaks.
q: Quadrupole carbon not clearly resolved.

Table 2
^{1}H NMR, ^{13}C NMR, Dept-135, HMBC, and HSQC-TOCSY data of Zagrosin II (**2**).

Position number	Hetero atom	^{1}H NMR	^{13}C NMR	Dept-135	HMBC (H → C)	HSQC-TOCSY
1	O	–	–	–	–	–
2		–	– (q)	–	–	–
3	O	–	–	–	–	–
4		–	– (q)	–	–	–
4a		–	– (q)	–	–	–
5		1.35	29.19 (s)	29.19	10, 9, 1′	1′, 6, 8, 7, 9, 10, 11
6		0.82, 1.34 §*	22.78 (s)	22.78	8, 10, 7	7, 5, 8, 1′
7		1.24§	23.54 (s)	23.54	6, 5	6, 5, 8, 9, 1′
8		0.82, 1.34 §*	30.65 (s)	30.65	11, 1′	11, 9, 7, 5, 6, 1′
8a		–	– (q)	–	–	–
9		1.68 §	38.53 (t)	38.53	1′, 5	1′, 10, 5, 7, 11
10		0.85	10.92 (p)	10.92	–	5, 6, 8, 9, 1′
11		1.25–1.32§*	14.03 (p)	14.03	5, 8	10, 6, 5,8
12	O	–	–	–	–	–
13		3.38	50.39 (p)	50.39	–	–
14	O	–	–	–	–	–
1′a		4.20 (dd)	68.18 (s)	68.18	–	10, 8, 7, 5, 6, 9
1′b		4.14 (dd)				
1″		–	132.36 (q)*	–	–	–
2″		7.60–7.65*	130.90 (t)*	130.90	6″, 2‴	3″, 4″, 5″, 6″
3″		7.43–7.45*	128.89 (t)*	128.89	6″, 5″	2″, 4″, 6″, 5″
4″		7.43–7.45*	128.89 (t)*	128.89	6″, 2″	2″, 3″,5″, 6″
5″		7.43–7.45*	128.89 (t)*	128.89	3″, 6″	3″, 2″, 4″, 6″
6″		7.60–7.65*	130.90 (t)*	130.90	2″, 2‴	2″, 3″,5″, 4″
1‴	O	–	–	–	–	–
2‴		–	167.95 (q)	–	–	–

§ Assigned and confirmed based on Dept-135, HMBC and HSQC-TOCSY data.
* Overlapped peaks.
q: Quadrupole carbon not clearly resolved.

solvent) sequentially. With consideration of the primary biological test results, 10 g of the methanolic extract was subjected to vacuum liquid chromatography (VLC) on 60 g of silica gel. As a mobile phase, *n*-hexane, chloroform, and methanol were used with the following gradient ratios: (*n*-hexane: chloroform, 10:20, 10:40, 10:80, 0:100, then chloroform: methanol, 10:10, 10:30, 10:50, 10:60, 10:80, 0:100) that yielded 10 fractions (fr$_{1-10}$). After performing toxicity assays on these fractions, the most active fractions (fr$_3$ and fr$_4$) were subjected to further purification steps using preparative thin layer chromatography (silica gel TLC) (Ebrahimi-Najafabadi et al. 2019) with chloroform: ethyl acetate: formic acid (5: 1: 0.5 v/v) as the mobile phases. As a result, Zagrosin I (**1**) (R$_f$ = 0.81, 124.0 mg) and Zagrosin II (**2**) (R$_f$ = 0.87, 172.6 mg) were purified from fr$_3$ and fr$_4$, respectively. 10 g of the hexane extract underwent silica gel VLC fractionation for Zagrosin III (3) isolation. As mobile phases, toluene (10 v/v), toluene: acetone (9:1 then 4:6 v/v), toluene: acetone: chloroform (6:4:2 then 2:4:4 v/v), and chloroform (10 v/v) were used, which yielded 6 fractions (fr$_{1-6}$). The fr$_1$ with the highest toxicity was purified using a preparative silica gel TLC with chloroform: ethyl acetate: acetic acid (8: 2: 0.1 v/v). As a result, 25 mg of Zagrosin III (**3**) with R$_f$ = 0.66 was isolated (Fig. S1 in Supplementary file no. 1).

2.3. MTT cytotoxicity assay

The cytotoxicity assay was performed as previously described (Hejr et al. 2017; Pasdaran et al. 2021; Azizi et al. 2021). The cytotoxicity was investigated on Human breast cancer (MCF-7), human fibrosarcoma (HT1080), and human foreskin fibroblast cells using the MTT (3-[4,5-dimethylthiazol-2-yl]-2,5 diphenyl tetrazolium bromide) assay. Cells were cultured in DMEM/F12, RPMI 1640-supplemented media with 10 % fetal bovine serum (FBS), and 100 IU/mL penicillin G. Incubation was done with 95 % air humidity and 5 % CO$_2$ at 37 °C. As a laboratory procedure, the cytotoxicity of different concentrations (2, 6.25, 12.5, 25, 50, 100, and 200 µg/mL) of isolated compounds was investigated by the colorimetric MTT method. As negative and positive controls, untreated cell cultures and paclitaxel were used, respectively. After the wells were incubated with MTT solution for 4 h, the absorbance of 24-, 48-, and 72-hour-treated cells with the isolated compounds was measured at 570 and 630 nm with an enzyme-linked immunosorbent assay (ELISA) plate

Table 3
¹H NMR, ¹³C NMR, Dept-135, HMBC, and HSQC-TOCSY data of Zagrosin III (**3**).

Position number	Hetero atom	¹H NMR	¹³C NMR	Dept-135	HMBC (H → C)	HSQC-TOCSY
1	O	–	–	–	–	–
2		–	–(q)	–	–	–
3	O	–	–	–	–	–
4		–	–(q)	–	–	–
4a		–	–(q)	–	–	–
5		1.68–2.31 §*	22.65 (s)	22.65	–	10, 11
6		1.68–2.31 §*	23.71 (s)	23.71	–	10, 11
7		1.68–2.31 §*	29.19 (s)	29.19	5	5, 6
8		1.68–2.31 §*	28.91 (s)	28.91	6	11, 6, 5
8a		–	–(q)	–	–	–
9		1.68 §	38.53 (t)	38.53	5	11, 5, 6, 7
10		0.85	10.94 (p)	10.94	9, 5	11, 5
11		1.31 §*	14.05 (p)	14.05	–	9, 5, 7, 8
12	O	–	–	–	–	–
13		3.38	50.39 (p)	50.39	–	–
14	O	–	–	–	–	–
1′a		4.20 (dd)	68.18 (s)	68.18	7, 9	10,7, 6, 8, 5
1′b		4.14 (dd)				
1″		–	167.01 (q)	–	–	–
2″		7.73 §*	129.01 (t)*	129.01	–	3″, 4″, 5″, 6″
3″		7.56 §*	130.82 (t)*	130.82	–	2″, 4″, 6″, 5″
4″		7.56 §*	129.01 (t)*	129.01	–	2″, 3″,5″, 6″
5″		7.56 §*	130.82 (t)*	130.82	–	3″, 2″, 4″, 6″
6″		7.73 §*	132.39 (t)*	132.39	–	2″, 3″,5″, 4″
1‴	O	–	–	–	–	–
1⁗	O	–	–	–	–	–
2‴		–	177.08 (q)*	177.08	–	–
3‴		2.19 §*	30.33 (s)	30.33	7‴, 6‴	4‴, 5‴
4‴		1.26 §	29.69 (s)	29.69	–	3‴, 5‴
5‴		1.26 §	31.45 (t)		–	3‴, 4‴
6‴		0.86–0.92 §*	20.97 (p)*	20.97	3‴, 4‴, 7‴	3‴,7‴
7‴		0.86–0.92 §*	20.97 (p)*	20.97	3‴, 4‴, 6‴	3‴,6‴

§ Assigned and confirmed based on Dept-135, HMBC and HSQC-TOCSY data.
* Overlapped peaks.
q: Quadrupole carbon not clearly resolved.

reader from BioTek Instruments®/USA (Deng et al. 2021; Pasdaran et al. 2022; Azizi et al. 2021). All experiments were performed in three replicates, and the data were presented as the percentage of growth inhibition.

2.4. Apoptosis assessment using annexin V-FITC/PI staining coupled with flow cytometry

For detection of apoptosis an FITC-Annexin V apoptosis detection kit (Cat No NBRA-001, MBR company, Iran) was used. The concentrations of Zagrosin I-III were selected based on the results of the MTT assays. After 24, 48, and 72 h of treatment of the cells by purified compounds (12.5 μg/mL of Zagrosin I, III or 25 μg/mL for Zagrosin II), they were washed, trypsinated, counted (each sample tube contained more than 50,000 cells) and prepared according to the manufacturer's instructions. Briefly after 3 washes, 500 μL of Annexin V-FITC binding buffer and 10 μL of FITC-conjugated Annexin V was added to the cells, and incubated for 15 min in dark condition. Subsequently, 2 μL of Propidium Iodide (PI) solution was added to each sample and incubated for 1–5 min in dark condition at room temperature. In each set of studied cell lines, negative control and induced apoptotic positive control were prepared. All prepared sample solutions were performed in triplicate and analyzed by flow cytometry using a flow cytometer (BD FACS Calibur with a 488-nm argon-ion laser). Cells of interest were gated; fluorescence was measured and the data of 10,000 cells were collected. Flowjo software was used to display the percent of normal and apoptotic cells. Normal cells and positive for FITC and/or PI cells were quantified by quadrant analysis and calculated. The data were represented as mean ± SD. As a detection tool, the apoptosis assay is used to establish the anticancer potential of any compound for tumor growth inhibition. In the resulted diagrams, the lower left quadrant displays the percentage of live cells (Annexin −V (−) /PI (−)), the lower right shows the percentage of early apoptotic cells (Annexin- V (+) /PI (−)), the upper right demonstrates late apoptotic and necrotic cells (Annexin- V (+) /PI (+), and the upper left shows secondary necrotic or dead cells (Annexin V-/PI +).

2.5. Cell cycle analysis

Cells (2×10^5 cells/mL) were exposed to control or isolated compounds)12.5 μg/mL of Zagrosin I, III or 25 μg/mL for Zagrosin II) for 6, 24, 48, and 72 h. In any case, after treatment, the cells were centrifuged at 5000 rpm for 15 min, and the supernatant was discarded. The cell pellets were washed twice in phosphate buffered saline (PBS) and centrifuged at 5000 rpm for 15 min (the supernatant was discarded), then fixed with 66 % ethanol on ice. The cell pellets were resuspended in staining solution based on the manufacturer's guidelines (ab139418 Propidium Iodide Flow Cytometry Kit for Cell Cycle Analysis; Abcam, Cambridge, UK). The resuspended cells were incubated at 37 °C in the dark for 20 min, then placed on ice and prepared for flow cytometry analysis. The effects of isolated compounds on cell cycle distribution were determined by a BD FACSCalibur™ Flow Cytometer (Becton, Dickinson and company, USA).

2.6. Structure elucidation

Nuclear Magnetic Resonance (NMR) spectra of the Isolated compounds were obtained in deuterated chloroform by a Bruker Ascend™ spectrometer (300 MHz for ¹H NMR, 75 MHz for ¹³C NMR, and 300 MHz for other techniques). 2D Pulse programs were selected from the Bruker software library. The δ scale (ppm) was used for all chemical shifts. A Waters Alliance 2695 HPLC Micromass Quattro micro-API Mass Spectrometer instrument with an Atlantis T3-C₁₈ 3μ, 2.1 × 100 mm column (35 °C temperature) and flow rate of 0.25 mL/min was used for LC-MS-MS analysis of isolated compounds. A linear gradient from 5–95 % acetonitrile in water was applied as the mobile phase for 15 min. For mass analysis (ESI positive mode), the following conditions were considered: cone voltage 35 V, extractor voltage 2 V, capillary voltage 4.5 kV, collision energy 45 eV, 200 L/h grade 5 N₂, 120 °C, and 300 °C for source and desolvation temperatures, respectively.

2.7. Statistical analysis

All data is represented as the mean ± standard deviation (SD) of at least 3 experiments. The IC_{50} (half-maximal inhibitory concentration) values in the cytotoxicity tests were calculated using GraphPad Prism version 8.0.2 (GraphPad Prism Software, San Diego, CA). Moreover, two-way analysis of variance (ANOVA) and Tukey's multiple comparison tests were used to compare the groups statistically. The significant level was considered $p \leq 0.05$. The two-way ANOVA not only aims to
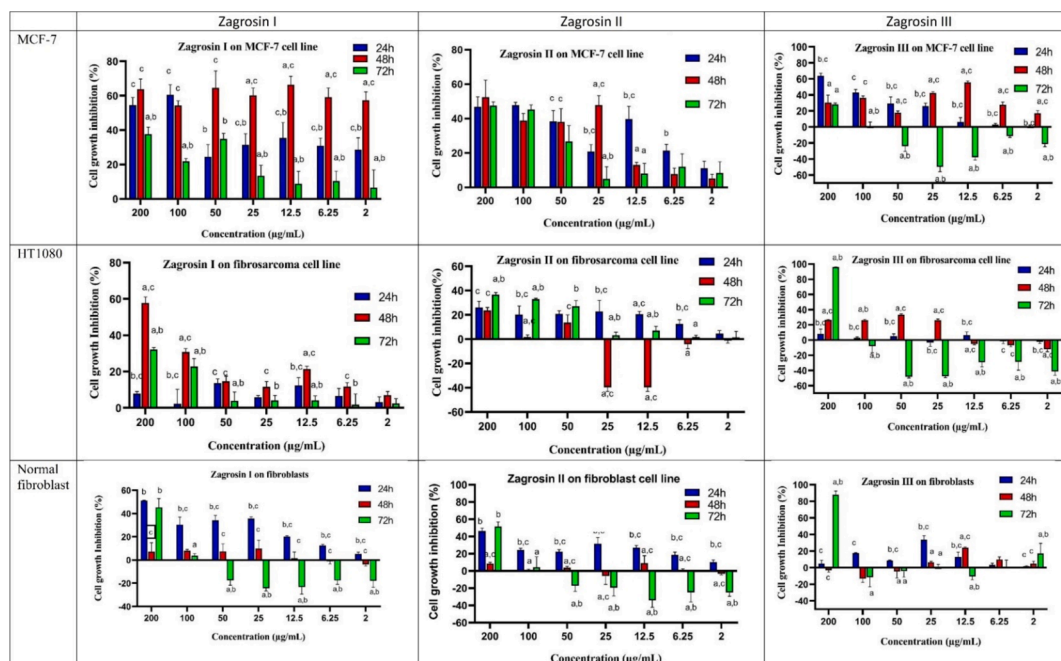
Fig. 2. The cytotoxic activity of Zagrosin I-III on MCF-7 normal human foreskin fibroblast, and human fibrosarcoma (HT1080) cells after 24 h, 48 h and 72 h of exposure, based on MTT assay. All experiments were performed in three replicates and the data were presented as the percentage of growth inhibition. Data are expressed as mean ± SD (a: significantly different from 24 h treated cells; b: significantly different from 8 h treated cells; c: significantly different from 72 h treated cells; $p < 0.05$).

assess the main effect of each independent variable, but also whether there is any interaction between them.

3. Results and discussion

3.1. Structural analysis

The structures of the three isolated compounds were elucidated based on NMR and LC-MS/MS data and are illustrated in Fig. 1.

The LC-MS chromatograms show the purity of the isolated compounds. For Zagrosin I (**1**), Zagrosin II (**2**), and Zagrosin III (**3**), the molecular weights were calculated as 404, 362, and 432 Dalton, respectively. Moreover, the fragmentation patterns based on LC-MS/MS data are presented to recheck the structure (Fig. S2 (Zagrosin I), Fig. S14 (Zagrosin II), and Fig. S26 (Zagrosin III) in Supplementary file no. 1).

Zagrosin I (**1**) is a pale-yellow amorphous compound. The ^{1}H NMR spectrum showed the presence of a benzoyl moiety [δ 7.7, 7.4, 8.2 ppm], a methine group at δ 1.6 ppm, a methoxy [δ 3.69 ppm], and a methylene [δ 4.2, 4.1 ppm] (Supplementary file no. 1).

As shown in Table 1, the HMBC and HSQC-TOCSY spectra assigned other protons, such as methyl moieties, H-11, and H-10 protons. The ^{13}C NMR spectrum exhibited the following signals: δ C 161.5, 167.8 ppm for two carbonyl groups, five methylene [δ C 28.9, 22.9, 23.6, 30.3, and 68.2 ppm], aromatic carbons [δ C128.7, 130.9, and 132.3 ppm], and two methyl groups [δ C14.0 and 10.9 ppm]. All carbons were also assigned based on Dept-135 spectrum signals (Table 1).

The backbone of compound (**1**) was assembled by interpreting the HMBC and HSQC-TOCSY spectra. The following proton-carbon correlations were observed in the HMBC spectrum: between H-5 (δ 1.35 ppm) and C-10 (δ C 10.9), C-1′ (δ C 68.2), C-7 (δ C 30.3), between H-1′ (δ 4.20, 4.14 ppm) and C-2‴ (δ C 161.5), C-9 (δ C 38.6), C-8 (δ C 30.3), C-5 (δ C 28.9), between H-11 (δ 1.2 ppm), and C-8 (δ C 30.31), C-5 (δ C 28.90).

The HSQC-TOCSY correlations between protons and carbon also showed how the proposed Zagrosin I (1) carbon backbone is connected, for example, between H-10 (δ 0.85 ppm) and H-6 (δ 0.82, 1.34), and H-1′ (δ 4.20), H-8 (δ 0.82, 1.34), and H-9 (δ 1.68). Additional data are noted

in Table 1 (Supplementary file no. 1). This compound with the formula of $C_{22}H_{28}O_7$ was elucidated as methyl (9)-8a-((benzoyloxy)methyl)-2-methoxy-4,9-dimethyltetrahydro-4H,5H-2,4a-methanobenzo[d] [1,3] dioxine-4-carboxylate and named Zagrosin I.

Zagrosin II (**2**) is a pale-yellow amorphous compound. The ^{1}H NMR spectrum showed a benzoyl moiety similar to the Zagrosin I [δ 7.6, 7.5, 7.9 ppm], a methoxy [δ 3.3 ppm], and a methylene [δ 4.2, 4.1 ppm]. Similar to the previous compound, Zagrosin I, other protons of Zagrosin II were authorized by HMBC and HSQC-TOCSY data. Subsequent structural information was obtained from the ^{13}C NMR spectrum: δ C 167.9 ppm for a carbonyl group, five methylene [δ C 29.1, 22.7, 23.5, 30.6, and 68.1 ppm], aromatic carbons [δ C128.8, 130.9, and 132.3 ppm], and two methyl groups [δ C14.0 and 10.9]. The Dept-135 spectrum as well as HMBC and HSQC-TOCSY signals, likewise to Zagrosin I, were used for all carbon assignments. In the HMBC spectrum, next proton-carbon correlations were detected: between H-5 (δ 1.34 ppm) and C-10 (δ C 10.9), C-1′ (δ C 68.1), C-9 (δ C 38.5), between H-11 (δ 1.25–1.32 ppm) and C-5 (δ C 29.1), and C-8 (δ C 30.6). The HSQC-TOCSY spectrum also revealed the following correlations: H-5 (δ 1.35 ppm) to H-1′ (δ 4.14, 4.20), H-8 (δ 0.82, 1.34), H-11 (δ 1.25–1.32), and H-1′ (δ 4.20, 4.14 ppm) to H-7 (δ 1.24), H-9 (δ 1.68), and H-5 (δ 1.35). Table 2 provides the detailed correlations.

More additional data were noted in Table 2, supporting information. Zagrosin II with the formula of $C_{20}H_{26}O_6$ seems to be a spirocyclic terpenoid and was elucidated as ((9)-4-hydroxy-2-methoxy-4,9-dimethyltetrahydro-4H,8aH-2,4-methanobenzo[d] [1,3] dioxin-8a-yl) methyl benzoate and named Zagrosin II.

Zagrosin III (**3**) is a pale-yellow amorphous compound. The ^{1}H NMR spectrum exhibited a phenyl moiety [δ 7.7, 7.5, 7.2 ppm], a methoxy [δ 3.3 ppm], five methyl groups [δ 1.3, 2.0, 0. HSQC-TOCSY 9 ppm], and a methylene group at δ 4.2 ppm. As with the above-maintained compounds, HSQC-TOCSY and HMBC data were also applied for Zagrosin III backbone structural elucidation. Other structural information was acquired from ^{13}C NMR and DEPT-135 spectra: a carbonyl group at δ C 177.0 ppm, seven methylene groups [δ C 68.8, 29.6, 30.3, 22.6, 23.7, 29.1, and 28.9 ppm], aromatic carbons [δ C129.0, 130.8, and 132.3
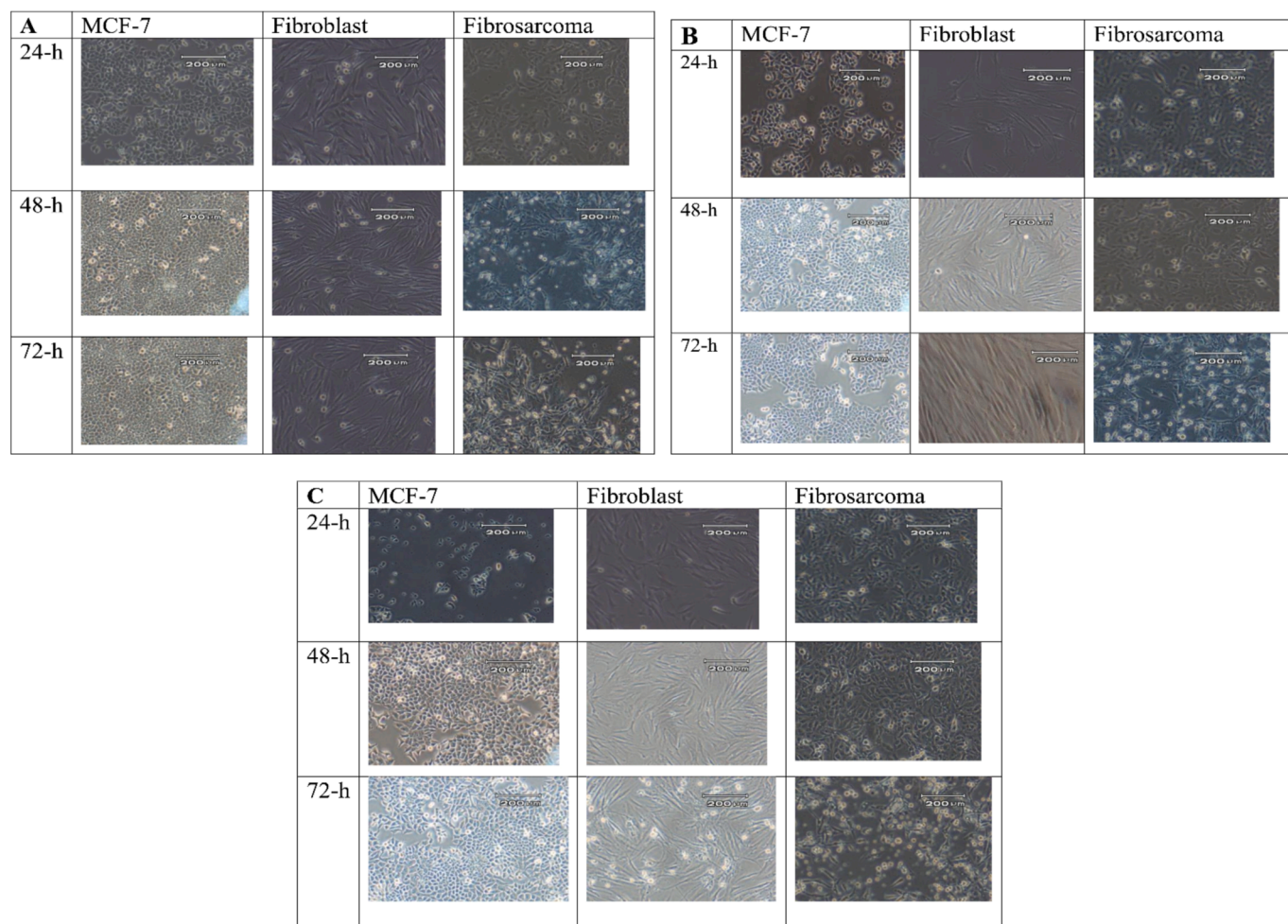
Fig. 3. Images of MCF-7, human fibrosarcoma (HT1080) and normal human foreskin fibroblasts cells in the culture medium, 24, 48, and 72 h after treatment with Zagrosin I (12.5 µg/mL, A), Zagrosin II (25 µg/mL, B), and Zagrosin III (12.5 µg/mL, C).

ppm], and four methyl groups [δ C14.0, 10.9, and 20.97 ppm]. Furthermore, from HMBC spectra, the following proton-carbon correlations were illustrated: between H-1′ (δ 4.14, 4.20 ppm) and C-7 (δ C 29.19), C-9 (δ C 38.53), and between H-10 (δ 1.3 ppm) and C-9 (δ C 38.53), and C-6 (δ C 22.65). The HSQC-TOCSY spectrum also revealed the following correlations: H-5 (δ 1.6–2.3 ppm) to H-10 (δ 0.85) and H-11 (δ 1.31); H-3⁗ (δ 2.1 ppm) to H-4⁗ and H-5⁗ (δ 1.26); and H-1′ (δ 4.14, 420 ppm) with H-10 (δ 1.3) and H-6 (δ 1.68–2.31). More additional data was noted in Table 3, supporting information. This compound with the formula of $C_{25}H_{36}O_6$ was elucidated as (9)-2-methoxy-4,9-dimethyl-8a-(phenoxy methyl) tetrahydro-4H,5H-2,4a-methanobenzo[d][1,3] dioxin-4-yl 4-methylpentanoate and named Zagrosin III.

Based on the backbone structure, compounds 1–3 belong to the substituted spirocyclic terpenoid class with a cyclic ether with a five-membered ether ring. The structures of Zagrosin I-II have similarities in acyl substitute (such as a benzoate ester) with (+)-Pedrolide which is a natural terpenoid that was first isolated from *Euphorbia pedroi*. Pedrolide is a diterpenoid with an unprecedented carbon skeleton, pedrolane, containing a bicycle[2.2.1]heptane system (Ferreira et al. 2020; Fadel and Carreira 2023).

Spiro compounds are molecules that have at least two molecular rings with only one common atom. Spirocyclic scaffolds are incorporated in various approved drugs and drug candidates (Hiesinger et al. 2020; Chupakhin et al. 2019). Spirocycles are thought to possess a good balance of conformational rigidity and flexibility to be, on one hand, free from absorption and permeability issues characteristic of conformationally more flexible, linear scaffolds. On the other hand, spirocycles

are more conformationally flexible compared to, for example, flat aromatic heterocycles and can adapt to many proteins as biological targets; thus, increasing the chances of finding bioactive hits (Chupakhin et al. 2019; Zheng, Tice, and Singh 2014). Zagrosin I-III which are isolated in the present study have spirocyclic terpenoid backbone. The following examples are closely related to our isolated compounds: polygalolide A, polygalolide B, 7-hydroxydehydroaustin, dehydroaustinol, austin, penicianstinoids A, penicianstinoids B, atrop-abyssomicin C, abyssomicin B, C, G, H, I (Fiedler 2021; Bai et al. 2019; Ma et al. 2003). A variety of biological activity including antiviral, antifungal and anticancer effects have been reported for some spirocyclic sesquiterpenes and sesquiterpenoids. As an example, illudin S is currently in Phase II clinical trials against ovarian, prostate, and gastrointestinal cancers (Chupakhin et al. 2019).

3.2. MTT cytotoxicity assay

This study was performed based on bioassay guided fractionation. All the obtained fractions and subfractions were tested for cytotoxicity applying MTT assay. The Zagrosins I-III were isolated as the major active compounds from the and most effective fractions (data not shown, Supplementary file no. 1). Different concentrations of the isolated compounds, Zagrosin I-III (1–3), showed different levels of cytotoxicity on 24, 48, and 72-h treated cell lines. The highest cytotoxicity was exhibited for Zagrosin I (1) on the human breast cancer cell line (MCF-7) after 24 h of exposure at 12.5 µg/mL (inhibition of MCF-7 cell proliferation was 66 %), 55.57 % inhibition at 12.5 µg/mL for Zagrosin III,
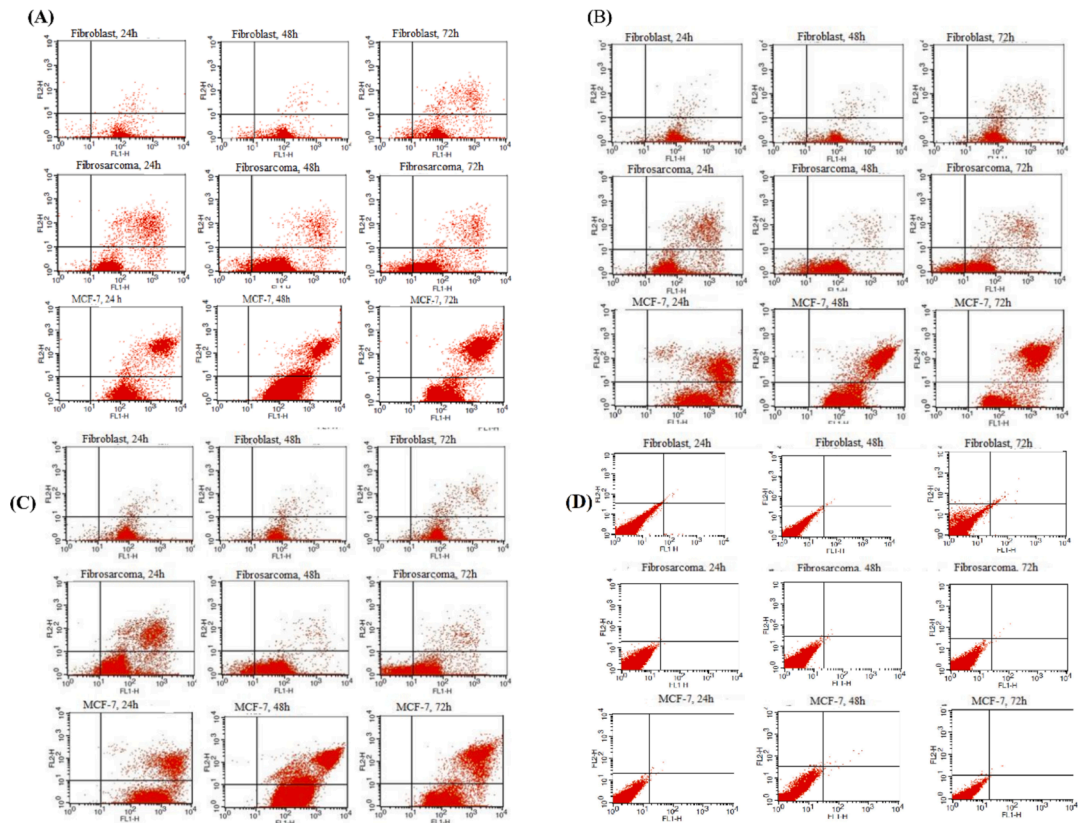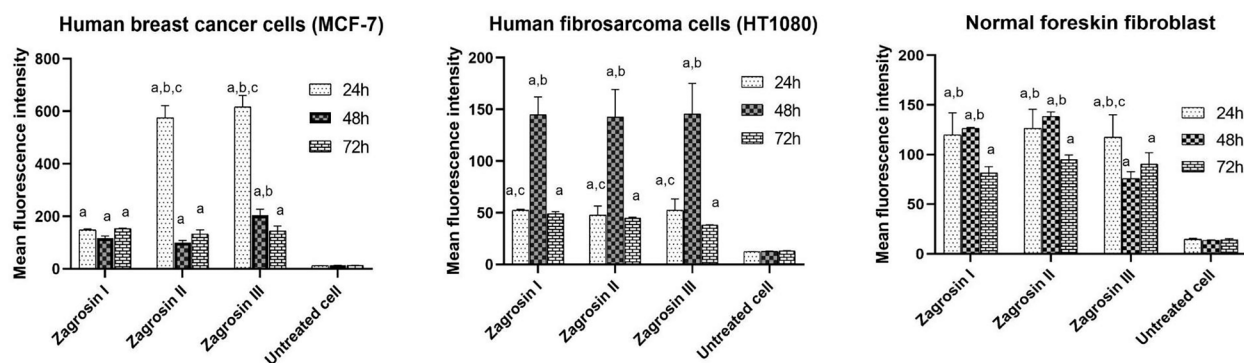
Fig. 4. Flow cytometric analysis diagram of the human fibrosarcoma (HT1080), MCF-7, and normal human foreskin fibroblast cell lines after 24 h, 48 h and 72 h of exposure to 12.5 µg/mL of Zagrosin I (A) and Zagrosin III (C) or 25 µg/mL of Zagrosin II (B), and untreated cells as the control (D). Each diagram can be divided into four separated regions include: (the lower left quadrant) percentage of live cells (Annexin V-/PI-), (the lower right quadrant) percentage of early apoptotic cells (Annexin V + /PI-), (the upper right quadrant) percentage of late apoptotic cells (Annexin V + /PI+), and (the upper left quadrant) percentage of necrotic cells (Annexin V-/PI+).
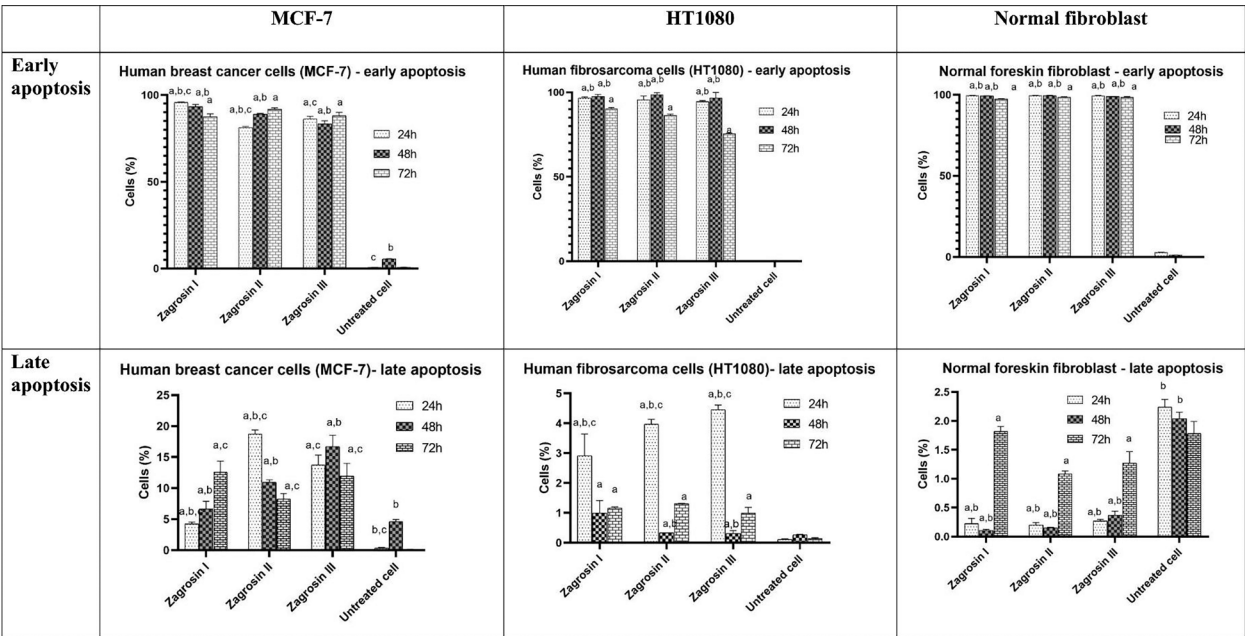
Fig. 5. The percentage of cells in early and late apoptosis based on flow cytometric results. Cells were treated with Zagrosin I-III for 24 h, 48 h and 72 h (12.5 µg/mL of Zagrosin I, III and 25 µg/mL of Zagrosin II). The data are presented as the mean ± SD (a: significantly different from untreated cells; b: significantly different from 72 h treated cells; c: significantly different from 48 h treated cells; $p < 0.05$).

Fig. 6. Comparison of the level of Mean Fluorescence Intensities of Zagrosin I-III induced late apoptosis in MCF-7, normal human foreskin fibroblast and human fibrosarcoma (HT1080). The median channels data were used for the measurement of the mean fluorescence intensity. Data of triplicate test are expressed as mean ± SD (a: significantly different with untreated cells; b: significantly different with 72 h treated cells; c: significantly different with 48 h treated cells; $p < 0.05$).

Table 4

Zagrosin I-III flow cytometric results of human fibrosarcoma (HT1080), MCF-7, and normal human foreskin fibroblast cells after 24 h, 48 h and 72 h of exposure at 12.5 μg/mL for Zagrosin I, III and 25 μg/mL for Zagrosin II. The data are presented as the mean ± SD.

| Cells (%)	Early apoptosis*			Late apoptosis*		
	Normal human foreskin fibroblast	Human fibrosarcoma cells (HT1080)	Human breast cancer cells (MCF-7)	Normal human foreskin fibroblast	Human fibrosarcoma cells (HT1080)	Human breast cancer cells (MCF-7)
Zagrosin I						
24 h	99.6 ± 0.049	96.56 ± 0.728	95.76 ± 0.317	0.225 ± 0.091	2.91 ± 0.728	4.23 ± 0.311
48 h	99.38 ± 0.097	97.63 ± 1.13	93.33 ± 1.244	0.105 ± 0.021	0.995 ± 0.417	6.66 ± 1.23
72 h	97.4 ± 0.169	90.41 ± 0.565	87.42 ± 1.781	1.82 ± 0.084	1.16 ± 0.042	12.57 ± 1.781
Zagrosin II						
24 h	99.61 ± 0.056	95.56 ± 2.19	81.24 ± 0.65	0.2 ± 0.042	3.97 ± 0.16	18.73 ± 0.65
48 h	99.45 ± 0.183	98.63 ± 1.074	89.025 ± 0.417	0.15 ± 0.014	0.34 ± 0.0	10.96 ± 0.41
72 h	98.67 ± 0.113	86.42 ± 0.671	91.74 ± 0.876	1.085 ± 0.049	1.3 ± 0.0141	8.26 ± 0.876
Zagrosin III						
24 h	99.47 ± 0.106	94.55 ± 0.565	86.23 ± 1.569	0.27 ± 0.028	4.45 ± 0.162	13.74 ± 1.59
48 h	98.91 ± 0.12	96.68 ± 3.196	83.28 ± 1.845	0.37 ± 0.07	0.315 ± 0.091	16.69 ± 1.84
72 h	98.4 ± 0.424	75.56 ± 0.365	88.005 ± 2.071	1.27 ± 0.197	0.995 ± 0.190	11.95 ± 2.04
Untreated cells						
24 h	2.86 ± 0.09	0.32 ± 0.04	0.62 ± 0.08	2.24 ± 0.13	0.11 ± 0.02	0.37 ± 0.08
48 h	1.12 ± 0.04	0.44 ± 0.06	5.53 ± 0.12	2.04 ± 0.11	0.27 ± 0.01	4.64 ± 0.31
72 h	0.30 ± 0.05	0.10 ± 0.02	0.69 ± 0.03	1.78 ± 0.21	0.14 ± 0.03	0.14 ± 0.02

*Statistical analysis of the data is presented in Fig. 5.

and then 55.57 % inhibition at 25 μg/mL for Zagrosin II.

As seen in Fig. 2, different concentrations of Zagrosin I-III (**1–3**) had a range of cytotoxicity on human fibrosarcoma (HT1080), MCF-7, and normal human foreskin fibroblast cell lines according to the MTT assay.

The highest cytotoxicity was observed in 48-h-treated MCF-7. The IC_{50} of Zagrosin I on 48-h-treated MCF-7 was calculated as 1.5 μg/mL. Zagrosin II and III exhibited cytotoxicity on 48-h-treated MCF-7 with IC_{50}s of 14.04 and 12.50 μg/mL, respectively. The IC_{50} of Zagrosin I on human fibrosarcoma (HT1080) was 115.5 μg/mL, Zagrosin III, 16.81 μg/mL (48 h treatment), and Zagrosin II, 142.7 μg/mL (72 h treatment). Zagrosin I and II stimulated cell proliferation of 72-h-treated normal foreskin fibroblasts at concentrations ≤ 100 μg/mL but inhibited the proliferation of 24-h-treated normal foreskin fibroblasts (30–40 %). Zagrosin I-III (**1–3**) didn't show significant cytotoxicity on 48-h-treated normal foreskin fibroblasts (lower than 10 %). Fig. 3 shows images of MCF-7, human fibrosarcoma (HT1080), and normal human foreskin fibroblast cells in the culture medium 24, 48, and 72 h after treatment with Zagrosin I, II, and III.

This study did not aim to estimate and quantify cell death kinetics. High-throughput time-lapse imaging is needed as well as mathematical modelling to capture the kinetics of cell death in terms of the length of time between the addition of a chemical substance and the onset of cell death and the maximum rate of this process within the population (Inde et al. 2020). It seems that there are differences in cell death kinetics between Zagrosins I-III, their concentrations, and cell lines. Based on the results of MTT assays we did not observe correlation between treatment times (24, 48 and 72 h) and the cell types (cancerous and normal cell line). This is not the first report on dose-independent and time-independent cytotoxicity of agents in the MTT assays against cancerous cell lines (Al-Qubaisi et al. 2011; Monzavi et al. 2019; Rosselli et al. 2012; Joseph et al. 2021). One can conjecture about some hypotheses. Initially, it is plausible that the chemical introduced into the culture media was taken up and processed by the cells within the first twenty-four hours (particularly at lower concentrations). After 48 and 72 h, the surviving cells began to multiply and make up for the loss because the cytotoxicity was not 100 %. The MTT assay's design and the metabolic alterations in specific cell lines may provide support for a different theory. Proliferation and cytotoxicity investigations both use the widely-recognized MTT test to determine the viable cell count. Enzymes known as NAD(P)H-dependent oxidoreductases, which are mostly located in the cytoplasm of cells, are responsible for the reduction of tetrazolium dye in the MTT test. In light of this, NAD(P)H flux-
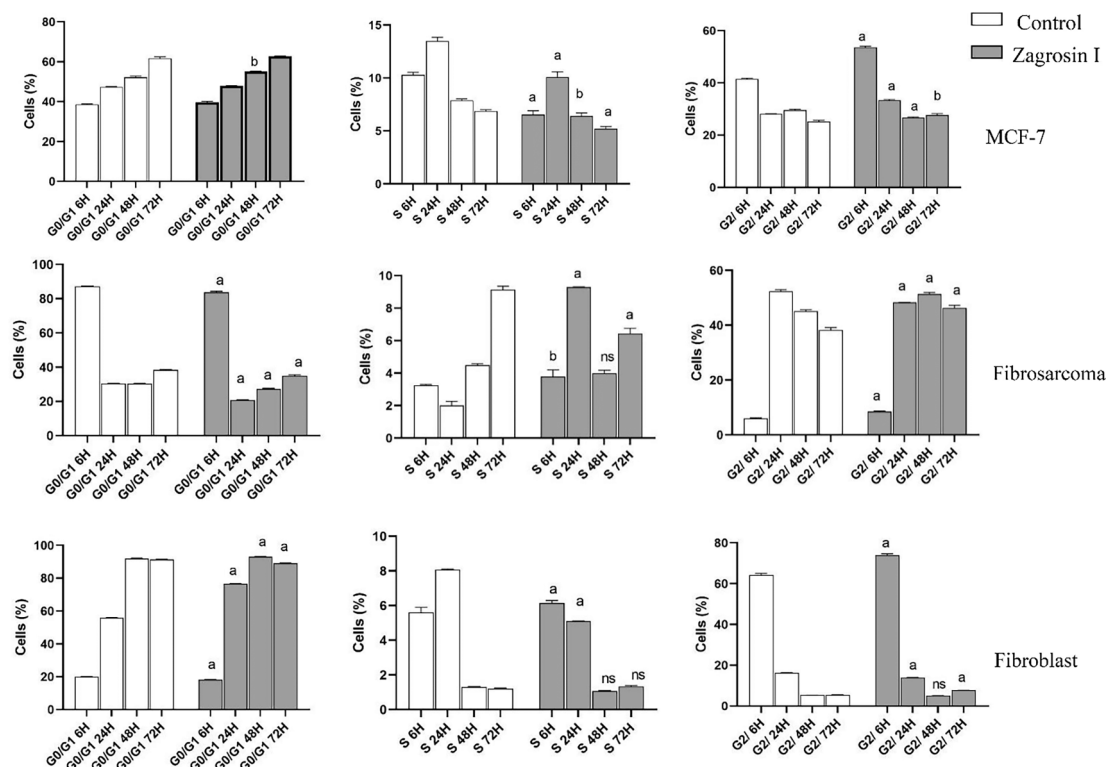
Fig. 7. Flow cytometric analysis of induced cell cycle arrest of MCF-7, human fibrosarcoma (HT1080), and normal human foreskin fibroblast cell lines after 6 h, 24 h, 48 h and 72 h of exposure at 12.5 μg/mL of Zagrosin I. Data of triplicate test are expressed as mean ± SD. Significant differences from the control (untreated cells) are shown at a: $p < 0.001$; b: $p < 0.05$.

related cellular metabolic activity is required for MTT dye elimination. Conversely, rapidly dividing cells diminish MTT at a substantial rate, while cells with a low metabolic rate reduce it relatively little. It is crucial to keep in mind that changes in metabolic activity during the MTT experiment might cause MTT dye decrease without compromising cell viability (Sylvester 2011; Stockert et al. 2012; Berridge, Herst, and Tan 2005; Azizi et al. 2021). It's also possible that this molecule stopped the cell cycle in the first 24 h, but the cells discovered a metabolic means to recover. By extending the duration to 72 h, the cells multiplied and made up for the initial decrease in MTT at the 24-hour time point (Azizi et al. 2021).
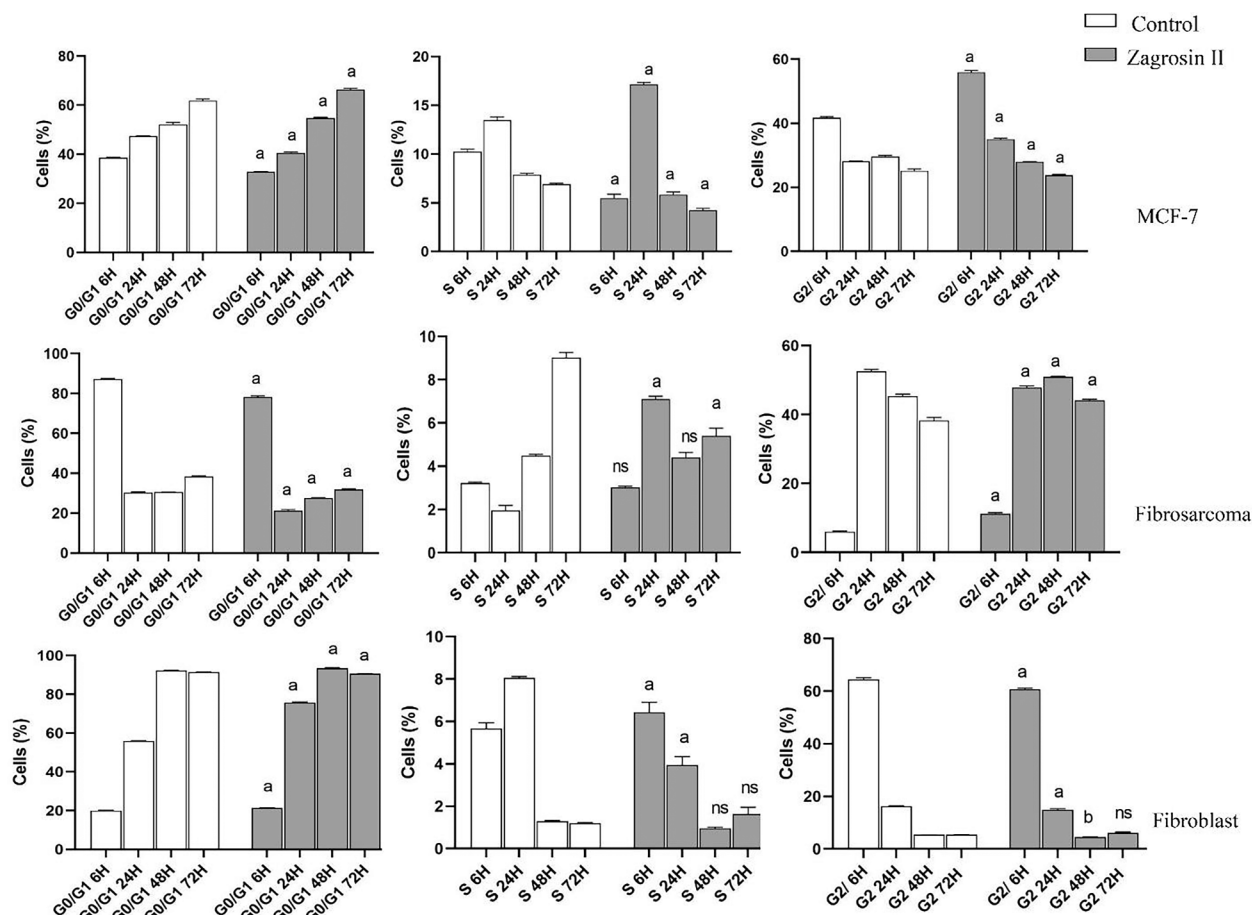
3.3. Flow cytometric analysis

Based on the FITC-Annexin V apoptosis flow cytometry assays, Zagrosin I-III (1–3) resulted in early apoptosis in more than 94 % of 24 and 48-h treated human fibrosarcoma (HT1080) and normal human foreskin fibroblast cells. Moreover, Zagrosin I resulted in early apotosis in 93–95 % of 24 and 48-h treated MCF-7 cells, while this effect for Zagrosin II and Zagrosin III was 81–89 %.

According to the results of flow cytometric analyses of late apoptosis in our study as shown in Figs. 4–6 and Table 4, the rate of late apoptosis in MCF-7 was more than two other cell lines during 3 studied times by treatment with Zagrosin I-III. Moreover, Regarding the analysis of mean fluorescence intensity (MFI) as shown in Fig. 6 the rate of phosphatidyl serine exposure which is reactive to Annexin V on the cell membrane of MCF-7 was more than two other studied cells due to the effect of Zagrosin I-III. It means that MCF-7 is more responsive to Zagrosin I-III at all studied time intervals in comparison to other studied cells. Besides, the cytotoxic effect of Zagrosin I on MCF-7 was increased during the time and was at the highest at 72 h of study. Whereas Zagrosin II and Zagrosin III were more effective on MCF-7 at 24 hrs. The late apoptosis in normal human foreskin fibroblast was significantly lower compared

to the untreated cells (control group).

A variety of natural molecules have been reported to exhibit anti-carcinogenic effects via various pathways, for instance, apoptosis, necroptosis, autophagy, mitotic catastrophe, mitochondrial processes, parthanatos, or paraptosis (Gali-Muhtasib et al. 2015; Luo et al. 2015; Sarkar and Li 2009). One of the most important biological routes is apoptosis, which plays a crucial role in homeostasis, the development, and the death of abnormal cells. A balance between cell proliferation and death is an important biological process in human body homeostasis; any dysregulation in this homeostasis could initiate various human malignancies. In many anti-cancer medications, drug-induced apoptosis is the predominant mechanism of action for cancer treatment. Several distinct stages, including G0/G1 (resting/first growth phases), S (synthesis phase), and G2/M (cell growth/mitotic phases), were distinguished in the human cell cycle. These cell cycle stages have specific checkpoints that show the quality and quantity of the cell cycle's major events such as the G0/G1 phase checkpoint (restriction point) and the G2/M checkpoint (DNA damage checkpoint). Cells will be arrested at G0/G1, S, and G2/M phases when DNA replicates and DNA damage needs to be repaired, respectively. Inducing apoptosis is common between various cytotoxic terpenoids. For example, lineariifolianoid E (a dimer isolated compound from the aerial parts of Inula lineariifolia Turcz.) showed a significant dose-dependent apoptosis effect in breast cancer cells (Qin et al. 2013). Other examples are: apoptotic effect of Pleuroton B (a bisabolane-type sesquiterpenoids isolated from the edible fungus Pleurotus cystidiosus O. K. Mill), Atractylenolide III (isolated from Atractylodes macrocephala Koidz. rhizome), Parviflorene F, an isolated sesquiterpenoid dimer from Curcuma parviflora Wall., with apoptotic effect via caspase-dependent mechanism, and Syringenes E and F (two dimeric eremophilane sesquiterpenoids isolated from Syringa pinnatifolia Hemsl. Stems) with apoptotic effect by activating ERK (Zheng et al. 2015; Kang et al. 2011; Ohtsuki et al. 2008; Li et al. 2022).

Fig. 8. Flow cytometric analysis of induced cell cycle arrest of MCF-7, human fibrosarcoma (HT1080), and normal human foreskin fibroblast cell lines after 6 h, 24 h, 48 h and 72 h of exposure at 25 μg/mL of Zagrosin II. Data of triplicate test are expressed as mean ± SD. Significant differencess from control (untreated cells) are shown at a: $p < 0.001$; b: $p < 0.05$.

3.4. Cell cycle analysis

The results of cell cycle analysis are shown in Figs. 7-9.

Zagrosin I

The number of MCF-7 cells treated with Zagrosin I significantly decreased in S phase (6–72 h), while there was a significant increase in the number of cells in G2 (6, 24, and 72 h after treatment).

In the case of the human fibrosarcoma (HT1080) cell line, the number of cells in Go/G1 decreased while the number of cells increased in S phase (6–24 h) and G2 phase (after 48 h).

Six hours after treatment, Zagrosin I increased the fibroblast cells in the S and G2 phases, but there was no significant difference at 48 h (Fig. 7).

Zagrosin II

In the case of MCF-7, there was a significant decrease in G0/G1 and S phases, while there was a significant increase in G2 phases 6 h after treatment. There was a significant increase in G0/G1 and decrease in the S and G2 phases 48 h after treatment. The number of human fibrosarcoma (HT1080) cells treated with Zagrosin II significantly increased in G0/G1 after 6 h, then decreased significantly. The number of these cells significantly increased in G2 (Fig. 8).

In the case of normal human foreskin fibroblast cells, 72 h after treatment, there was no significant difference between control and Zagrosin II-treated cells in the S and G2 phases (Fig. 8).
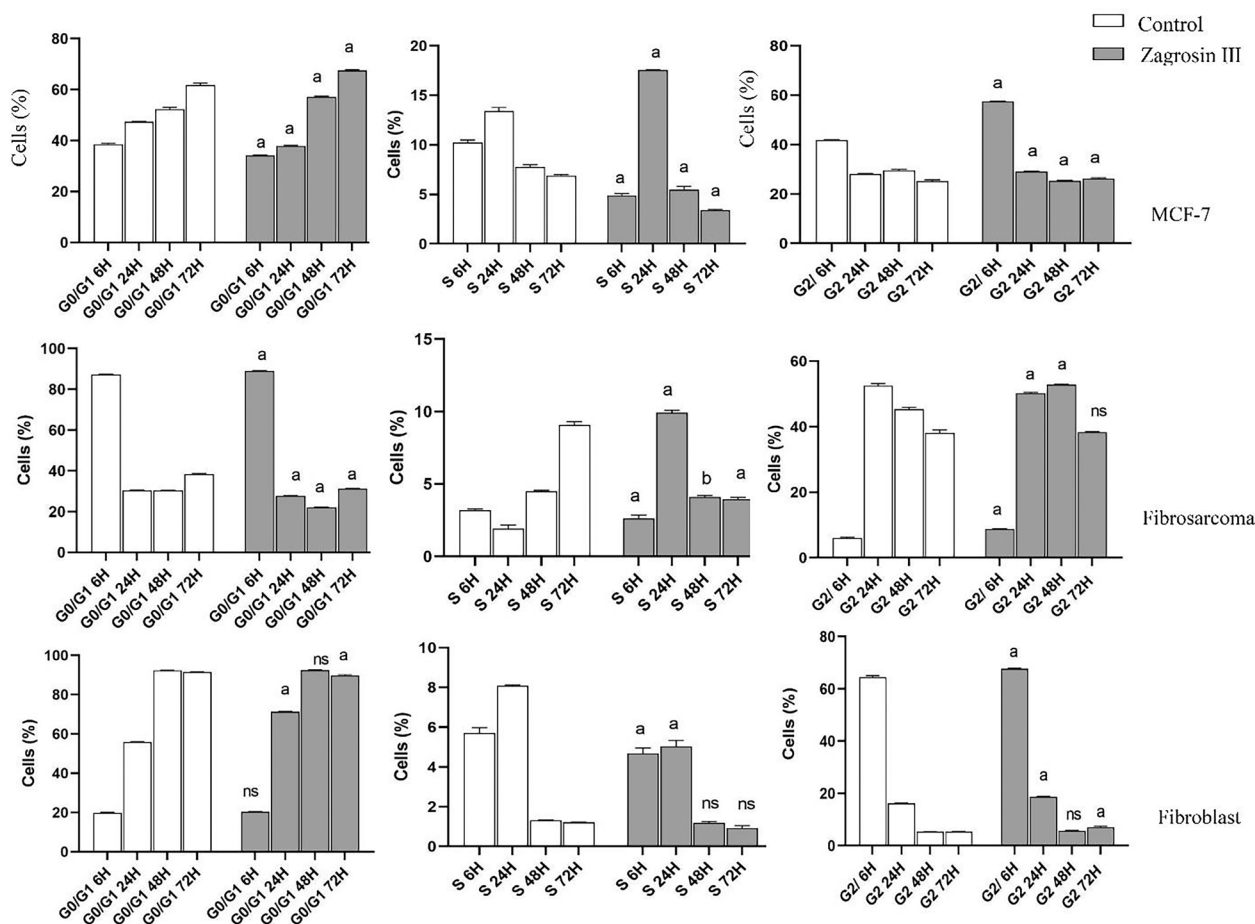
Zagrosin III

The number of MCF-7 cells treated with Zagrosin III significantly decreased in G0/G1 and S phases (6 h), while there was a significant increase in the number of cells in S and G2 (24 h after treatment).

In the case of the human fibrosarcoma (HT1080) cell line, the number of cells in Go/G1 significantly decreased while the number of cells increased in S phase (24 h) and G2 phase (after 48 h). In the case of normal human foreskin fibroblast cells, 48 h after treatment, there was no significant difference between control and Zagrosin III-treated cells in the S and G2 phases (Fig. 9).

Based on the observed results, the isolated compounds (Zagrosin I–III) induced late apoptosis on cancerous cell lines, MCF-7 and HT1080 while the late apoptosis in normal human foreskin fibroblast was significantly lower compared to the untreated cells (control group). Moreover, the isolated compounds (Zagrosin I–III) are not necrotic, but they induce early apoptotic changes such as cell shrinkage and apoptotic bodies, and cell morphological changes reflect this cell death type (Sun et al. 2010). Similar cell changes were reported accompanied by other natural anti-carcinogenic molecules, e.g., epigallocatechin-3-gallate, celastrol, protopanaxadiol Rg3 and Rh2, yessotoxin, and bleomycin (Wang et al. 2012; Gupta et al. 2004; Korsnes and Espenes 2011; Han et al. 2020; Li et al. 2020).

We had some limitations in this study; for instance, at this stage we could not provide HRMS spectra, and we only relied on LC-MS/MS data and NMR spectra. Moreover, we could not determine the absolute configuration of the molecules through X-ray crystallography. We could only determine the cytotoxicity through MTT assays and the involvement of apoptosis as one of the mechanisms that these molecules applied to exhibit this cytotoxicity through flow cytometric analysis. But to evaluate antitumor and anticancer properties, further *in vivo* studies are required.

Fig. 9. Flow cytometric analysis of induced cell cycle arrest of MCF-7, human fibrosarcoma (HT1080), and normal human foreskin fibroblast cell lines after 6 h, 24 h, 48 h and 72 h of exposure at 12.5 μg/mL of Zagrosin II. Data of triplicate test are expressed as mean ± SD. Significant differences from the control (untreated cells) are shown at a: $p < 0.001$; b: $p < 0.05$.

4. Conclusion

In this study, 3 new cytotoxic spirocyclic terpenoids from *E. amygdaloides* L were isolated and structurally elucidated. These cytotoxic compounds include (9)-8a-((benzoyloxy)methyl)-2-methoxy-4,9-dimethyltetrahydro-4H,5H-2,4a-methanobenzo[d] [1,3] dioxine-4-carboxylate (Zagrosin I), ((9)-4-hydroxy-2-methoxy-4,9-dimethylte-trahydro-4H,8aH-2,4a-methanobenzo[d] [1,3] dioxin-8a-yl) methyl benzoate (Zagrosin II), and (9)-2-methoxy-4,9-dimethyl-8a-(phenoxy methyl) tetrahydro-4H,5H-2,4a-methanobenzo[d][1,3]dioxin-4-yl 4-methylpentanoate (Zagrosin III). These compounds exhibited significant cytotoxicity against the MCF-7 cell line and human fibrosarcoma (HT1080), with the mechanism of early and late apoptosis affecting cells mostly in G0/G1 followed by S, and G2 phases. Regarding the mean fluorescence intensity, the rate of phosphatidyl serine exposure on the cell membrane of MCF-7 was more than two other studied cells due to the effect of Zagrosin I-III which indicated that MCF-7 is more responsive to Zagrosin I-III at all studied time intervals in comparison to other studied cells. The cytotoxicity of these compounds on normal human foreskin fibroblasts was low 48 h after treatments. Although to evaluate antitumor and anticancer properties, further *in vivo* studies are required, this study showed that these spirocyclic terpenoids from *E. amygdaloides* can be considered as an effective chemical backbone for developing new anticancer agents.

CRediT authorship contribution statement

Ardalan Pasdaran: Writing – review & editing, Writing – original draft, Supervision, Methodology, Formal analysis, Data curation, Conceptualization. **Negar Azarpira:** Writing – review & editing, Validation, Supervision, Methodology, Investigation, Data curation, Conceptualization. **Mahdokht Hossein Aghdaie:** Writing – review & editing, Writing – original draft, Visualization, Validation, Supervision, Methodology, Investigation, Formal analysis, Data curation. **Maryam Zare:** Writing – review & editing, Methodology, Investigation, Data curation. **Negin Sheidaie:** Writing – review & editing, Methodology, Investigation, Formal analysis, Data curation. **Fatemeh Hajeb Fard:** Writing – review & editing, Methodology, Investigation, Formal analysis, Data curation. **Azadeh Hamedi:** Writing – review & editing, Writing – original draft, Visualization, Validation, Supervision, Software, Resources, Project administration, Methodology, Investigation, Funding acquisition, Formal analysis, Data curation, Conceptualization.

Declaration of competing interest

The authors declare that they have no known competing financial interests or personal relationships that could have appeared to influence the work reported in this paper.

Acknowledgments

This study was part of the Pharm. D thesis projects of Negin Sheidaie and Fatemeh Hajeb Fard, part of the author team of this manuscript.

Appendix A. Supplementary data

Supplementary data to this article can be found online at https://doi.org/10.1016/j.arabjc.2024.106049.

Data availability

Data will be made available on request.

References

Al-Qubaisi, M., Rozita, R., Yeap, S.-K., Omar, A.-R., Ali, A.-M., Alitheen, N.B., 2011. Selective cytotoxicity of goniothalamin against hepatoblastoma HepG2 cells. Molecules 16 (4), 2944–2959.

Amtaghri, S., Akdad, M., Slaoui, M., Eddouks, M., 2022. Traditional uses, pharmacological, and phytochemical studies of Euphorbia: A review. Curr. Top. Med. Chem. 22 (19), 1553–1570.

Azizi, K., Hamedi, A., Azarpira, N., Hamedi, A., Shahini, M., Pasdaran, A., 2021. A new cytotoxic sesquiterpene lactone from *Euphorbia microsphaera* Boiss against human breast cancer (MCF-7) and human fibrosarcoma (HT1080) cells. Toxicon 202, 60–66.

Bai, M., C.-J. Zheng, G.-L. Huang, R.-Q. Mei, B. Wang, Y.-P. Luo, C. Zheng, Z.-G. Niu, and G.-Y. Chen. 2019. Bioactive meroterpenoids and isocoumarins from the mangrove-derived fungus *Penicillium sp.* TGM112. *J. Nat. Prod.* 82 (5):1155-1164.

Barile, E., Corea, G., Lanzotti, V., 2008. Diterpenes from Euphorbia as potential leads for drug design. Na Prod Commun 3 (6), 1934578X0800300629.

Benjamaa, R., Moujanni, A., Kaushik, N., Choi, E.H., Essamadi, A.K., Kaushik, N.K., 2022. Euphorbia species latex: A comprehensive review on phytochemistry and biological activities. Front. Plant Sci. 13, 1008881.

Berridge, M.V., Herst, P.M., Tan, A.S., 2005. Tetrazolium dyes as tools in cell biology: new insights into their cellular reduction. Biotechnol. Annu. Rev. 11, 127–152.

Chupakhin, E., Babich, O., Prosekov, A., Asyakina, L., Krasavin, M., 2019. Spirocyclic Motifs in Natural Products. Molecules 24 (22).

Corea, G., Fattorusso, C., Fattorusso, E., Lanzotti, V., 2005. Amygdaloidins A-L, twelve new 13 α-OH jatrophane diterpenes from Euphorbia amygdaloides L. Tetrahedron 61 (18), 4485–4494.

Deng, J., Hu, J., Zhao, J., An, N., Liang, K., Wang, Q., Zhang, Z., Wu, R., Zhang, F., 2021. Eco friendly synthesis of fluorescent carbon dots for the sensitive detection of ferric ions and cell imaging. Arab. J. Chem. 14 (7), 103195.

Ebrahimi-Najafabadi, H., Kazemeini, S.S., Pasdaran, A., Hamedi, A., 2019. A novel similarity search approach for high-performance thin-layer chromatography (HPTLC) fingerprinting of medicinal plants. Phytochem. Anal 30 (4), 405–414.

Ernst, M., Grace, O.M., Saslis-Lagoudakis, C.H., Nilsson, N., Simonsen, H.T., Rønsted, N., 2015. Global medicinal uses of Euphorbia L. (Euphorbiaceae). J. Ethnopharmacol. 176, 90–101.

Fadel, M., Carreira, E.M., 2023. Enantioselective Total Synthesis of (+)-Pedrolide. J. Am. Chem. Soc. 145 (15), 8332–8337.

Ferreira, R.J., Spengler, G., Orthaber, A., Dos Santos, D.J., Ferreira, M.-J.-U., 2020. Pedrolane, a polycyclic diterpene scaffold containing a bicyclo [2.2. 1] heptane system, from *Euphorbia pedroi*. Org. Lett. 23 (2), 274–278.

Fiedler, H.-P., 2021. Abyssomicins—A 20-Year Retrospective View. Mar. Drugs 19 (6), 299.

Gali-Muhtasib, H., Hmadi, R., Kareh, M., Tohme, R., Darwiche, N., 2015. Cell death mechanisms of plant-derived anticancer drugs: beyond apoptosis. Apoptosis 20 (12), 1531–1562.

Gupta, S., Hastak, K., Afaq, F., Ahmad, N., Mukhtar, H., 2004. Essential role of caspases in epigallocatechin-3-gallate-mediated inhibition of nuclear factor kappaB and induction of apoptosis. Oncogene 23 (14), 2507–2522.

Hamedi, A., Bayat, M., Asemani, Y., Amirghofran, Z., 2022. A review of potential anti-cancer properties of some selected medicinal plants grown in Iran. J. Herb. Med. 33, 100557.

Han, Q., Han, L., Tie, F., Wang, Z., Ma, C., Li, J., Wang, H., Li, G., 2020. (20S)-Protopanaxadiol Ginsenosides Induced Cytotoxicity via Blockade of Autophagic Flux in HGC-27 Cells. Chem. Biodivers. 17 (7), e2000187.

Hejr, H., Ghareghani, M., Zibara, K., Ghafari, M., Sadri, F., Salehpour, Z., Hamedi, A., Negintaji, K., Azari, H., Ghanbari, A., 2017. The ratio of 1/3 linoleic acid to alpha linolenic acid is optimal for oligodendrogenesis of embryonic neural stem cells. Neurosci. Lett. 651, 216–225.

Hiesinger, K., Darin, D., Proschak, E., Krasavin, M., 2020. Spirocyclic scaffolds in medicinal chemistry. J. Med. Chem. 64 (1), 150–183.

Inde, Z., Forcina, G.C., Denton, K., Dixon, S.J., 2020. Kinetic Heterogeneity of Cancer Cell Fractional Killing. Cell Rep. 32 (1), 107845.

Joseph, J., Khor, K.Z., Moses, E.J., Lim, V., Aziz, M.Y., Abdul Samad, N., 2021. In vitro Anticancer Effects of Vernonia amygdalina Leaf Extract and Green-Synthesised Silver Nanoparticles. Int. J. Nanomed. 16, 3599–3612.

Kang, T.-H., Bang, J.-Y., Kim, M.-H., Kang, I.-C., Kim, H.-M., Jeong, H.-J., 2011. Atractylenolide III, a sesquiterpenoid, induces apoptosis in human lung carcinoma A549 cells via mitochondria-mediated death pathway. Food Chem. Toxicol. 49 (2), 514–519.

Kemboi, D., Peter, X., Langat, M., Tembu, J., 2020a. A Review of the Ethnomedicinal Uses, Biological Activities, and Triterpenoids of Euphorbia Species. In. Molecules.

Kemboi, D., Peter, X., Langat, M., Tembu, J., 2020b. A review of the ethnomedicinal uses, biological activities, and triterpenoids of Euphorbia species. Molecules 25 (17), 4019.

Korsnes, M.S., Espenes, A., 2011. Yessotoxin as an apoptotic inducer. Toxicon 57 (7–8), 947–958.

Li, A., Jiao, S., Huang, H., Chen, P., Zhang, R., Su, G., Xu, J., Liu, C., Hu, Z., Chen, S., Tu, P., Chai, X., Huang, L., 2022. Syringenes A-L: Bioactive dimeric eremophilane sesquiterpenoids from *Syringa pinnatifolia*. Bioorg. Chem. 125, 105879.

Li, X., Kim, S.E., Chen, T.Y., Wang, J., Yang, X., Tabib, T., Tan, J., Guo, B., Fung, S., Zhao, J., 2020. Toll interacting protein protects bronchial epithelial cells from bleomycin-induced apoptosis. FASEB J. 34 (8), 9884–9898.

Luo, X., Yu, X., Liu, S., Deng, Q., Liu, X., Peng, S., Li, H., Liu, J., Cao, Y., 2015. The role of targeting kinase activity by natural products in cancer chemoprevention and chemotherapy. Oncol. Rep. 34 (2), 547–554.

Ma, W., Wei, X., Ling, T., Xie, H., Zhou, W., 2003. New phenolics from Polygala fallax. J. Nat. Prod. 66 (3), 441–443.

Magozwi, D.K., Dinala, M., Mokwana, N., Siwe-Noundou, X., Krause, R.W., Sonopo, M., McGaw, L.J., Augustyn, W.A., Tembu, V.J., 2021. Flavonoids from the genus euphorbia: Isolation, structure, pharmacological activities and structure–activity relationships. Pharmaceuticals 14 (5), 428.

Moghaddas, E., Khamesipour, A., Mohebali, M., Fata, A., 2017. Iranian native plants on treatment of cutaneous leishmaniasis: a narrative review. Iran. J. Parasitol. 12 (3), 312.

Monzavi, N., Zargar, S.J., Gheibi, N., Azad, M., Rahmani, B., 2019. Angiopoietin-like protein 8 (betatrophin) may inhibit hepatocellular carcinoma through suppressing of the Wnt signaling pathway. Iran. J. Basic Med. Sci. 22 (10), 1166–1171.

Müller, R., Pohl, R., 1970. Flavonol glycosides of Euphorbia amygdaloides and their quantitative determination at various stages of plant development. 5. Flavonoids of native Euphorbiaceae. Planta Med. 18 (2), 114–129.

Ogbourne, S.M., Parsons, P.G., 2014. The value of nature's natural product library for the discovery of new chemical entities: the discovery of ingenol mebutate. Fitoterapia 98, 36–44.

Ohtsuki, T., Tamaki, M., Toume, K., Ishibashi, M., 2008. A novel sesquiterpenoid dimer parviflorene F induces apoptosis by up-regulating the expression of TRAIL-R2 and a caspase-dependent mechanism. Bioorg. Med. Chem. 16 (4), 1756–1763.

Özbilgin, S., Gülçin, S., 2012. Uses of some Euphorbia species in traditional medicine in Turkey and their biological activities *Turk*. J. Pharm. Sci. 9 (2).

Pascal, O.A., Bertrand, A.E.V., Esaïe, T., Sylvie, H.-A.-M., Eloi, A.Y., 2017. A review of the ethnomedical uses, phytochemistry and pharmacology of the Euphorbia genus. Pharma Innov. 6 (1, Part A), 34.

Pasdaran, A., Azarpira, N., Yaghoobi Solut, N., Zare, M., Hamedi, A., Karami, N., Hamedi, A., 2022. Cytotoxic properties, anthocyanin and furanocoumarin content of red-pigments obtained from *Callistemon citrinus* (Curtis) skeels flowers. Res. J. Pharmacog. 8 (4), 79–90.

Pasdaran, A., Azarpira, N., Heidari, R., Nourinejad, S., Zare, M., Hamedi, A., 2022. Effects of some cosmetic dyes and pigments on the proliferation of human foreskin fibroblasts and cellular oxidative stress; potential cytotoxicity of chlorophyllin and indigo carmine on fibroblasts. J. Cosmet. Dermatol. 21 (9), 3979–3985.

Qin, J.-J., Jin, H.-Z., Huang, Y., Zhang, S.-D., Shan, L., Voruganti, S., Nag, S., Wang, W., Zhang, W.-D., Zhang, R., 2013. Selective cytotoxicity, inhibition of cell cycle progression, and induction of apoptosis in human breast cancer cells by sesquiterpenoids from *Inula lineariifolia* Turcz. Eur. J. Med. Chem. 68, 473–481.

Rosselli, S., Bruno, M., Raimondo, F.M., Spadaro, V., Varol, M., Koparal, A.T., Maggio, a., 2012. Cytotoxic effect of eudesmanolides isolated from flowers of Tanacetum vulgare ssp. siculum. Molecules 17 (7), 8186–8195.

Sarkar, F.H., Li, Y., 2009. Harnessing the fruits of nature for the development of multi-targeted cancer therapeutics. Cancer Treat. Rev. 35 (7), 597–607.

Stockert, J.C., Blázquez-Castro, A., Cañete, M., Horobin, R.W., Villanueva, Á., 2012. MTT assay for cell viability: Intracellular localization of the formazan product is in lipid droplets. Acta Histochem. 114 (8), 785–796.

Sun, Q., Chen, T., Wang, X., Wei, X., 2010. Taxol induces paraptosis independent of both protein synthesis and MAPK pathway. J. Cell. Physiol. 222 (2), 421–432.

Sylvester, P.W., 2011. Optimization of the tetrazolium dye (MTT) colorimetric assay for cellular growth and viability. In: Drug Design and Discovery. Springer, pp. 157–168.

Wang, W.B., Feng, L.X., Yue, Q.X., Wu, W.Y., Guan, S.H., Jiang, B.H., Yang, M., Liu, X., Guo, D.A., 2012. Paraptosis accompanied by autophagy and apoptosis was induced by celastrol, a natural compound with influence on proteasome, ER stress and Hsp90. J. Cell. Physiol. 227 (5), 2196–2206.

Zhao, H., Sun, L., Kong, C., Mei, W., Dai, H., Xu, F., Huang, S., 2022. Phytochemical and pharmacological review of diterpenoids from the genus Euphorbia Linn (2012–2021). J. Ethnopharmacol. 298, 115574.

Zheng, Y., Tice, C.M., Singh, S.B., 2014. The use of spirocyclic scaffolds in drug discovery. Bioorganic Med. Chem. Lett. 24 (16), 3673–3682.

Zheng, Y., Pang, H., Wang, J., Shi, G., Huang, J., 2015. New apoptosis-inducing sesquiterpenoids from the mycelial culture of Chinese edible fungus *Pleurotus cystidiosus*. J. Agric. Food Chem. 63 (2), 545–551.